Journal of Inflammation Research

Dovepress
Taylor & Francis Group

Open Access Full Text Article

ORIGINAL RESEARCH

# Identification of *RSAD2* as a Key Biomarker Linking Iron Metabolism and Dendritic Cell Activation in Systemic Lupus Erythematosus Through Bioinformatics and Experimental Validation

Hengrong Qian[1,*], Sheng Gao[2,*], Ting Zhang[3,*], Yuanyuan Xie[4,*], Siyan Chen[5,*], Yanggang Hong[1,*], Xinlei Wu[1], Zhouhang Xing[4], Lingjie Kong[1], Jintao Mo[6], Yiming Lin[6], Anzhe Zheng[1], Wenqian Wang[7], Liangxing Wang[8], Chunyan Hua[4]

[1]School of the 2nd Clinical Medical Sciences, Wenzhou Medical University, Wenzhou, Zhejiang Province, People's Republic of China; [2]Laboratory Animal Center, Wenzhou Medical University, Wenzhou, Zhejiang Province, People's Republic of China; [3]Department of Rheumatology, The First Affiliated Hospital of Wenzhou Medical University, Wenzhou, Zhejiang Province, People's Republic of China; [4]School of Basic Medical Sciences, Wenzhou Medical University, Wenzhou, Zhejiang Province, People's Republic of China; [5]School of Ophthalmology & Optometry, School of Biomedical Engineering, Wenzhou Medical University, Wenzhou, Zhejiang Province, People's Republic of China; [6]School of the 1st Clinical Medical Sciences, Wenzhou Medical University, Wenzhou, Zhejiang Province, People's Republic of China; [7]Department of Plastic Surgery, The Second Affiliated Hospital and Yuying Children's Hospital of Wenzhou Medical University, Wenzhou, Zhejiang Province, People's Republic of China; [8]Key Laboratory of Heart and Lung, Division of Pulmonary Medicine, The First Affiliated Hospital of Wenzhou Medical University, Wenzhou, Zhejiang Province, People's Republic of China

*These authors contributed equally to this work

Correspondence: Chunyan Hua, School of Basic Medical Sciences, Wenzhou Medical University, Wenzhou, Zhejiang Province, 325035, People's Republic of China, Tel/Fax +86-577-86689769, Email huachunyan@wmu.edu.cn; Liangxing Wang, Key Laboratory of Heart and Lung, Division of Pulmonary Medicine, The First Affiliated Hospital of Wenzhou Medical University, Wenzhou, Zhejiang Province, 325035, People's Republic of China, Email wangliangxing@wzhospital.cn

**Background:** Systemic lupus erythematosus (SLE) is characterized by aberrant immune activation and disrupted iron metabolism, yet the molecular mediators that govern both processes remain unclear. This study aims to identify pivotal genes that modulate immune responses and iron metabolism, and to delineate their contributions to SLE pathogenesis.

**Methods:** Differentially expressed genes related to iron metabolism (IM-DEGs) were identified using datasets (GSE72326, GSE110169, GSE126307, and GSE50772) from the GEO database and the MSigDB. Functional enrichment analyses were performed on the iron metabolism related genes (IM-Genes). A weighted gene co-expression network analysis was constructed to identify hub genes, which were further refined as potential biomarkers using the least absolute shrinkage and selection operator method. The predictive value of these biomarkers was validated using receiver operating characteristic (ROC) curves and the nomogram. CIBERSORT was employed to evaluate immune cell infiltration in SLE. Additionally, the expression and function of *RSAD2* were confirmed using RNA interference, quantitative real-time PCR, and Western blotting techniques.

**Results:** Bioinformatics analyses identified 4 potential biomarkers: *RSAD2, MT2A, LCN2*, and *LTF. RSAD2* exhibited the highest clinical validity (AUC = 0.927) and was closely associated with classic diagnostic indicators. Its diagnostic potential was confirmed through ROC curve and nomogram, highlighting its role in SLE pathogenesis. Elevated *RSAD2* expression was observed in peripheral blood mononuclear cells of SLE patients, positively correlating with activated dendritic cells (DCs). Notably, *Rsad2* knockdown markedly impaired the function of activated DCs, as evidenced by suppressed expression of inflammatory mediators and iron metabolism-related genes.

**Conclusion:** Our findings suggest that *RSAD2* is a potential diagnostic biomarker and therapeutic target for SLE, elucidating the intricate relationship between immune dysregulation and aberrant iron metabolism in activated DCs, which exacerbates SLE.

**Keywords:** systemic lupus erythematosus, dendritic cell, iron metabolism, biomarker, *RSAD2*, inflammation



Received: 23 October 2024
Accepted: 27 February 2025
Published: 14 March 2025

# Introduction

Systemic lupus erythematosus (SLE) is a chronic autoimmune disorder characterized by heterogenous manifestations.[1] The pathogenesis of SLE is complex, involving the breakdown of immune tolerance, which leads to the production of autoantibodies, formation of immune complexes, and their deposition in multiple organs.[2,3] Recent studies have demonstrated a positive correlation between elevated interferon (IFN) signatures and increased SLE activity, as well as higher autoantibody levels. Notably, approximately 60% to 80% of SLE patients exhibit upregulated expression of IFN-stimulated genes (ISGs).[4] Dendritic cells (DCs), as the most potent antigen-presenting cells, play a pivotal role in initiating autoimmune responses and maintaining immune tolerance. Overactivation of DCs can trigger inflammatory mediators, disrupt the balance between effector and regulatory T cells, and lead to sustained B cell activation and autoantibody production.[5]

Systemic and intracellular iron homeostasis is essential for numerous biological procedures, including energy metabolism, DNA synthesis, oxidative stress management, and cellular respiration. This balance is maintained through the coordinated regulation of iron absorption, utilization, storage, recycling, and export.[6] Disruption of iron metabolic homeostasis is frequently observed in SLE. For instance, many SLE patients exhibit clinical signs resembling iron deficiency anemia due to decreased serum iron levels.[7] Conversely, iron overload has been identified within the renal tissues of patients with lupus nephritis (LN), highlighting the complexity and variability of iron homeostasis alterations in SLE.[8] Emerging evidence suggests that disturbances of iron metabolism within immune cells contribute to SLE pathogenesis.[8–10] Although previous studies have highlighted the critical role of DCs in initiating autoimmune responses, the interplay between iron metabolism and DCs activation in the context of SLE remains poorly understood. Additionally, specific biomarkers for iron metabolism disorders in SLE are lacking, and little is known about genes that could simultaneously regulate immune response and iron metabolism in SLE.

This study aims to identify key biomarkers associated with iron metabolism in SLE by analyzing raw data from the Molecular Signatures Database (MSigDB) and the Gene Expression Omnibus (GEO) database. Through bioinformatics analyses, we pinpointed *RSAD2* as the key biomarker and validated its expression and protein levels in clinical samples. Our findings highlight the critical role of *RSAD2* in iron metabolism and the activation of DCs. Notably, this research underscores the potential of *RSAD2* in predicting iron metabolism disorders linked to immune dysregulation in SLE, thereby offering new insights into the mechanisms of SLE and paving the way for innovative therapeutic strategies.

# Materials and Methods

## Data Acquisition and Processing

Microarray datasets, GSE72326 was retrieved from the NCBI GEO database (http://www.ncbi.nlm.nih.gov/geo/).[11] This dataset, based on the GPL10558 platform (Illumina HumanHT-12 V4.0 expression beadchip), comprised 157 SLE blood samples and 20 healthy control (HC) samples (Table 1). Detailed information regarding samples in this dataset was provided in the Supplementary Table S1. Probe annotations were converted to corresponding gene symbols using platform-specific annotation files.

## Identification of DEGs

The GEO2R web application (http://www.ncbi.nlm.nih.gov/geo/geo2r), which employs the "limma" R package (v3.54.0), was used to identify differentially expressed genes (DEGs) between SLE patients and HCs. Genes lacking official gene symbol or with multiple probe sets were excluded from the subsequent analysis. The criteria for DEGs were determined with $p < 0.05$ and $|\log_2 FC| > 1$.[12] Volcano plots and heatmaps were generated using "ggplot2" and "pheatmap" R packages to visualize the DEGs.

**Table 1** Dataset Information From GEO Database

| Dataset | Sample Size | Platform |
|---|---|---|
| GSE72326 | 177 (comprising 20 hC and 157 SLE samples) | GPL10558 platform (Illumina HumanHT-12 V4.0 expression beadchip) |
| GSE110169 | 155 (comprising 82 RA and 73 SLE samples) | GPL13667 platform (Affymetrix Human Genome U219 Array) |
| GSE50772 | 81 (comprising 20 hC and 61 SLE samples) | GPL570 platform ([HG-U133_Plus_2] Affymetrix Human Genome U133 Plus 2.0 Array) |
| GSE126307 | 40 (comprising 9 hC and 31 SLE samples) | GPL13369 platform (Illumina Human Whole-Genome DASL HT) |

**Abbreviations**: HC, healthy control; SLE, systemic lupus erythematosus; RA, rheumatoid arthritis.

## Identification of Iron Metabolism Related Genes

A total of sixteen gene sets related to iron metabolism were curated from the MSigDB (http://software.broadinstitute.org/gsea/index.jsp), yielding 514 unique genes after removing duplicates (Supplementary Table S2).[13] A Venn diagram[14] was utilized to separately perform the intersection between dataset genes and iron metabolism gene lists by "ggVennDiagram" R package, resulting in the identification of 124 iron metabolism-related genes (IM-Genes) in SLE.

## Functional Annotation and Pathway Enrichment Analyses

Gene Ontology (GO) enrichment analysis was performed using the "clusterProfiler" R package, encompassing biological process (BP), cellular component (CC) and molecular function (MF) domains. Results were visualized using the "ggplot2" and "GOplot" R packages. Kyoto Encyclopedia of Genes and Genomes (KEGG) pathway analysis was conducted using FunRich 3.1.3 (http://www.funrich.org/). Statistical significance was set at $p < 0.05$ for both GO and KEGG analyses.

## Construction of WGCNA

The weighted gene co-expression network analysis (WGCNA) was performed using the "WGCNA" R package to construct co-expression networks of genes from GSE72326. Briefly, a correlation matrix was generated using the Pearson correlation coefficients, which was then transformed into a weighted adjacency matrix using an appropriate soft-thresholding power. The pickSoftThreshold function is utilized to assist in the selection of the soft threshold. This adjacency matrix was converted to a topological overlap matrix (TOM), and genes were clustered into modules based on TOM dissimilarity using average-linkage hierarchical clustering. Closely related modules were merged, and module eigengenes (MEs) were calculated as the first principal component of each module. Module-trait relationships were determined based on correlations between gene modules and clinical traits. Hub genes associated with iron metabolism in SLE were identified as those with the highest intramodular connectivity. The "ggVennDiagram" R package was utilized to identify overlapping biomarkers.

## Identification and Validation of Potential Biomarkers

The 124 IM-Genes were further analyzed using the LASSO logistic regression algorithm implemented in the "glmnet" package of R software.[15] The LASSO model parameters were set as follows: alpha = 1; maximum iterations (max_iter): 500; data normalisation was not performed; and the coefficient update method was cyclic.

To identify candidate genes with high sensitivity and specificity for SLE diagnosis, ROC curves of 4 IM-DEGs were generated and the area under the curve (AUC) was calculated using the "pROC" package in R.[16] An AUC value of 0.5–0.7 indicates a low diagnostic effect, 0.7–0.9 suggests a moderate effect, and above 0.9 indicates a high diagnostic accuracy. For further validation, we employed an independent dataset GSE110169 (GPL13667 platform, Affymetrix Human Genome U219 Array) comprising 82 rheumatoid arthritis (RA) and 73 SLE samples (Table 1). A risk model was constructed using logistic regression, and its performance visualized through a nomogram generated with the "regplot" R package.[17] Model calibration predictive performance was assessed by generating a calibration curve.

## Evaluation of Immune Cell Infiltration

We estimated the relative proportions of infiltrating immune cells using the Cell-type Identification By Estimating Relative Subsets Of RNA Transcripts (CIBERSORT) package in R (https://cibersort.stanford.edu/)[18] on the LM22 gene signature file from CIBERSORT and immune cell markers from PanglaoDB (https://panglaodb.se/index.html). Differences in immune cell composition between the HC and SLE groups were compared, with statistical significance set at $p < 0.05$. The "ggplot2" package was used to visualize the results.

## Immune Correlation Analysis

The "corrplot" R package was utilized to analyze the correlation between the expression of RSAD2 and the proportion of immune cells. A correlation diagram was created with the "ggplot2" R package to illustrate the immune relationships between *RSAD2* and specific immune cells. Statistical significance was set at $p < 0.05$. The correlation of 4 IM-DEGs with immune cells was determined using the cor function and visualized using the "pheatmap" package.

## Validation of the Hub Genes Expression

To validate the expression of the hub genes in SLE, datasets GSE126307 (platform GPL13369, Illumina Human Whole-Genome DASL HT) and GSE50772 (platform GPL570, [HG-U133_Plus_2] Affymetrix Human Genome U133 Plus 2.0 Array) were analyzed. The detailed information of the two datasets could be found in Table 1. Data visualization was conducted using the "ggpubr" R package to generate box plots.

## Ethics Approval

This study was conducted in accordance with the Declaration of Helsinki and received approved from the Clinical Research Ethics Committee of the First Affiliated Hospital of Wenzhou Medical University. All participants provided signed informed consent forms. The Issuing Number is KY2023-083. All experiments using mice were approved by the Institutional Animal Care and Use Committee at Wenzhou Medical University (Animal Welfare Assurance), the approval number for animal ethics is xmsq2022-0792 and complied with the National Institutes of Health Guide for the Care and Use of Laboratory Animals.

## Human Subjects and Clinical Protocol

Clinical samples were collected from the First Affiliated Hospital of Wenzhou Medical University between January and December 2023. All patients met the American College of Rheumatology revised criteria for the classification of SLE.[19] The SLE disease activity index 2000 (SLEDAI-2K) was assessed at the time of blood sampling.[20] Detailed clinical features of the participants are available in Table 2. PBMCs were isolated from peripheral blood using Ficoll density gradient centrifugation.

**Table 2** Clinical Patients Information and Related Immune Molecules

| Characteristics | SLE | HC |
|---|---|---|
| Number of cases | 46 | 20 |
| Age, Mean ± SD (years) | 36.45 ± 7.11 | 30.48 ± 5.39 |
| Sex ratio (male: female) | 1:8 | 1:6 |
| C3 (g/L) | 0.69 ± 0.08 | 1.18 ± 0.6 |
| C4 (g/L) | 0.13 ± 0.17 | 0.35 ± 0.74 |
| IgG (g/L) | 18.35 ±4.37 | 9.21 ± 2.81 |
| Albumin (g/L) | 45.3 ± 6.6 | 42.7 ± 5.9 |
| BUN (mmol/L) | 6.5 ± 1.2 | 3.4 ± 0.9 |
| Creatinine (μmol/L) | 112 ± 17 | 46 ± 3 |

**Abbreviations**: SLE, systemic lupus erythematosus; HC, healthy control; C3, complement component 3; IgG, immunoglobulin G; BUN, blood urea nitrogen.

## Primary Dendritic Cell Culture

Female C57BL/6 mice, aged 4–6 weeks, were purchased from Beijing Vital River Laboratory Animal Technology Co., Ltd. These mice were maintained under specific pathogen-free (SPF) conditions, with a 12-hour light-dark cycle. A minimum acclimation period of one week was allowed before any experimental procedures were conducted. Bone marrow-derived dendritic cells (BMDCs) were generated from femoral and tibial bone marrow progenitor cells. Following harvest, cells underwent erythrocyte lysis using a buffer provided by Solarbio (Beijing, China). These cells were then seeded in 12-well plates at a density of $1\times10^6$ cells/mL in RPMI 1640 medium supplemented with 10% heat-inactivated fetal bovine serum, 10 ng/mL recombinant GM-CSF and 10 ng/mL recombinant IL-4 (PeproTech, Rocky Hill, NJ, USA). Half of the medium was replaced every 2 days. By day 6, non-adherent and loosely adherent cells were collected for further experimental use. All cell cultures were incubated at 37 °C in a humidified 5% $CO_2$ incubator.

## RNA Interference

Small interfering RNA (siRNA) targeting murine *Rsad2* and negative control siRNA (scrambled siRNA) were designed and synthesized by RiBoBio (Guangzhou, China). The sequences of *Rsad2* siRNA were as follows: sense, 5′-GCAGAAAGAUUUCUUAUAA-3′; antisense, 5′-UUAUAAGAAAUCUUUCUGC-3′. BMDCs were seeded in 6-well plates and stimulated with 1 μg/mL lipopolysaccharide (LPS; Sigma-Aldrich, St. Louis, MO, USA) for 24 h. Cells were then transfected with 200 nM siRNA using Lipofectamine 3000 (Invitrogen, Carlsbad, CA, USA) according to the manufacturer's instructions. Knockdown efficiency was assessed by RT-qPCR and Western blot analysis 24 h post-transfection.

## RNA Extraction and RT-qPCR

Total RNA was extracted from cells using Trizol reagent (Takara, Shiga, Japan) according to the manufacturer's instructions. RNA quality and concentration were assessed at 260/280 nm using a NanoDrop spectrophotometer (Thermo Fisher Scientific, Waltham, MA, USA). One microgram of RNA was reverse-transcribed to cDNA according to the kit (Vazyme, Nanjing, Chian). Quantitative real-time PCR was performed using ChamQ SYBR Green Master Mix (Vazyme). The primer sequences were as follows: *Rsad2*, forward 5′-ACCCTCCTACCTCAACTCCAAG-3′, and reverse 5′-CCATCCAACTGACCACATCCAT-3′; *β-actin, forward* 5′-TCAAGATCATTGCTCCTCCTGAG-3′, and reverse 5′-ACATCTGCTGGAAGGTGGACA-3′. The cycling conditions were: 95°C for 30s, followed by 40 cycles of 95°C for 10s, and 60°C for 30s. Relative gene expression was calculated using the 2^-ΔΔCt method, where the fold difference = $2^{-(\Delta Ct \text{ of the target gene-}\Delta Ct \text{ of the reference gene})} = 2^{-\Delta\Delta Ct}$. The normalized value for *RSAD2* mRNA expression were calculated as the relative quantity of *RSAD2* divided by the relative quantity of β-actin. All samples were run in triplicate.

## Western Blotting

Cells were lysed in RIPA buffer (Beyotime, Shanghai, China) supplemented with 1 mm PMSF. Protein concentrations were determined using a BCA Protein Kit (Beyotime, Shanghai, China). Equal amounts of protein were separated by 12% SDS-PAGE and transferred to PVDF membranes (Millipore, Burlington, MA, USA). Membranes were blocked with 5% non-fat milk in TBST for 1h at room temperature and then incubated with primary antibodies (1:2000) overnight at 4°C. After washing, membranes were incubated with HRP-conjugated secondary antibodies (1:3000, Affinity Biosciences, Cincinnati, OH, USA) for 1 h at room temperature. Protein bands were visualized using an enhanced chemiluminescence kit (Vazyme) and imaged using an Amersham Imager 680 (GE Healthcare, Chicago, IL, USA). Band intensities were quantified using Image J software (National Institutes of Health, Bethesda, MD, USA).

## Statistical Analysis

Statistical analyses were conducted using R software (version 4.3.2) (https://www.r-project.org/) and the relevant R packages (http://www.bioconductor.org/). Continuous variables were analyzed using Student's *t*-test or one-way

ANOVA with Tukey's post hoc test for multiple comparisons. Correlations were assessed using Spearman's rank correlation coefficient. $P < 0.05$ was considered statistically significance. Data are presented as mean ± standard deviation (SD) from at least three independent experiments. GraphPad Prism 8 (GraphPad Software, San Diego, USA) was used for data visualization.

# Results

## Identification and Biological Enrichment Analyses of DEGs

Figure 1 depicts the comprehensive workflow of our study. Utilizing high-throughput transcriptomic analysis, we utilized dataset GSE72326 from the GEO database, ultimately identifying 4950 genes with $p$-value < 0.05. The GSE72326 dataset[21] comprises 177 samples, including 157 SLE patients and 20 hCs (Supplementary Table S1). With the threshold of $|\log_2 FC| > 1$ and $p$-value < 0.05, we identified 100 DEGs (90 up-regulated, 10 down-regulated). These DEGs were visually represented in the volcano plots (Figure 2A). A heatmap was generated to display the expression patterns of the top 10 upregulated and top 10 downregulated genes with the most statistical significance (Figure 2B). The comprehensive list of all DEGs were listed in Supplementary Table S3.

Subsequently, GO and KEGG pathway enrichment analyses were performed to explore the functional implications of the 4950 genes. GO analysis highlighted key BP, MF and CC terms, particularly focusing on immune response regulation. Significant GO terms include those related to the regulation of innate immune response, response to type I IFN, cellular response to type I IFN, and IFN-mediated signaling pathways, as detailed in the chord diagram (Figure 2C) (Supplementary Table S4). The KEGG pathway enrichment analysis further emphasized the involvement of critical immune pathways, notably IFN-α/β signaling, and cytokine signaling in the immune system. These biological pathways were associated with significant $p$-values and effect sizes (Figure 2D), supporting the central role of these genes in the dysregulation of immune responses in SLE pathogenesis.

## Identification of Key Gene Modules Associated With SLE Progression by WGCNA

To elucidate the gene modules relevant to the progression of SLE, we applied WGCNA to the GSE72326 dataset. Initial clustering of all samples facilitated the inclusion of relevant data for subsequent analysis (Figure 3A). The optimal soft-threshold power was determined to be $\beta = 12$, achieving a scale-free topology fit index $R^2 = 0.9$, which confirmed the scale-free network distribution of gene connectivity (Figure 3B). A hierarchical clustering tree was constructed using the TOM, resulting in the identification of eight distinct gene modules after merging those with similar expression profiles (Figure 3C). Each module was assigned a unique color for ease of identification. The correlation analysis conducted between these modules and clinical traits demonstrated a statistically significant correlation with the clinical characteristics of SLE. Specifically, the blue, brown, red, and yellow modules exhibited statistically significant correlations with SLE ($p < 0.05$), as depicted in module-trait heatmap (Figure 3D). Notably, the MEbrown module demonstrated the strongest positive correlation with SLE, with a correlation coefficient of 0.53. Further analysis using a scatter plot confirmed correlation between the brown module and SLE (r = 0.7, $p$ = 7.3e–34) (Figure 3E), comprising 221 genes (Supplementary Table S5).

## Identification and Functional Enrichment of IM-Genes in SLE

We initially screened 514 iron metabolism genes from the MSigDB database (Supplementary Table S3). To identify the overlapping results between two databases, a Venn analysis was conducted. Of the 4950 genes identified in SLE ($p < 0.05$), 124 were found to overlap with IM genes, termed IM-Genes (Figure 4A). GO enrichment analysis of the 124 IM-Genes revealed their involvement in key terms including mitochondrial membrane composition, iron-sulfur cluster binding, and metal ion binding, implicating their potential roles in both iron metabolism and mitochondrial dysfunction in SLE (Figure 4B) (Supplementary Table S4). Further KEGG enrichment analysis highlighted significant involvement in pathways related to iron uptake and transport, xenobiotic metabolism, and transferrin endocytosis, underscoring the importance of iron homeostasis in SLE pathogenesis (Figure 4C). To narrow down critical IM-Genes, we intersected the IM gene set with the top 100 DEGs in SLE ($p < 0.05$, $|\log_2 FC| > 1$) and WGCNA modules (blue, brown, red, and

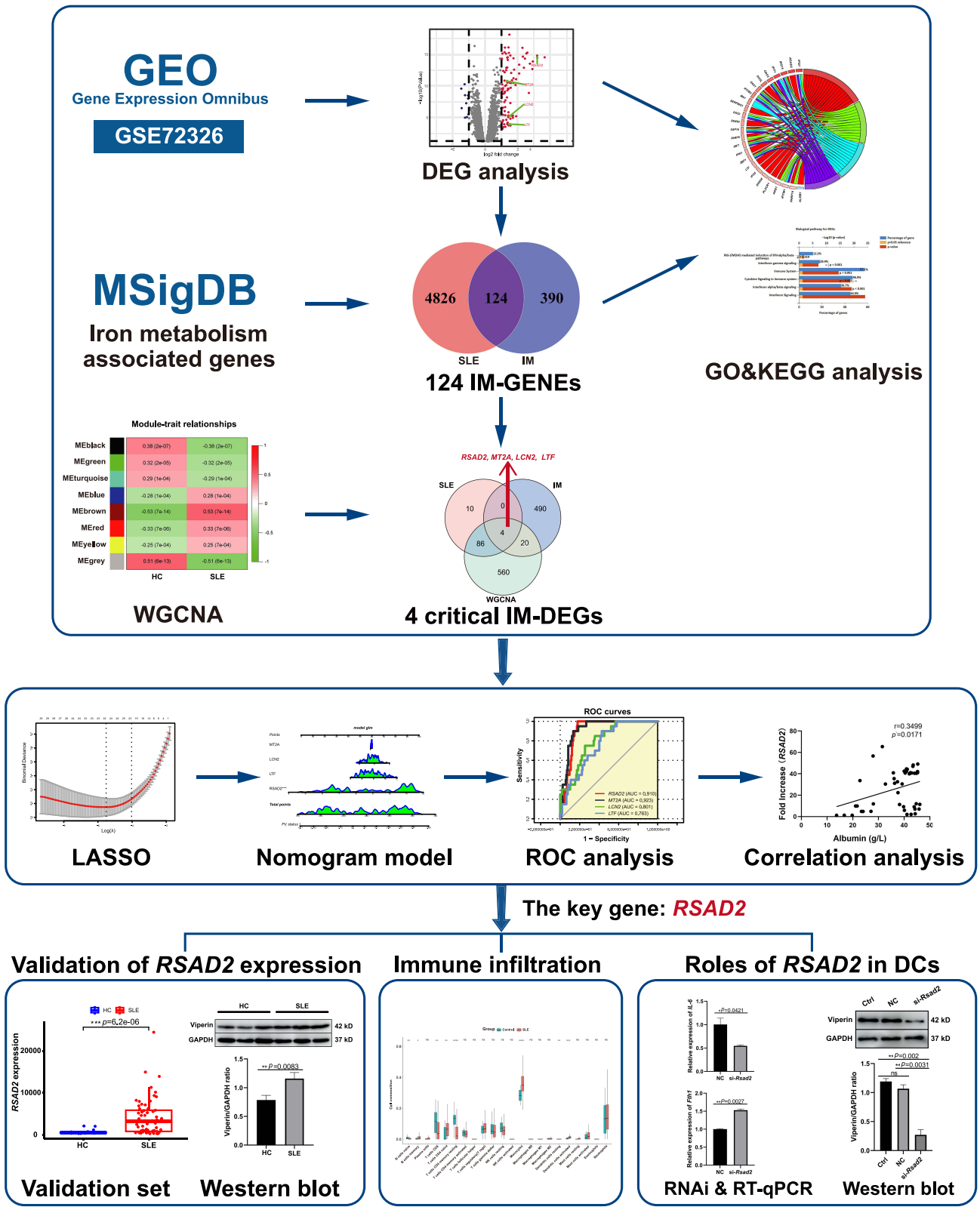


**Figure 1** Workflow of the study. *$p$ < 0.05, **$p$ < 0.01, ***$p$ < 0.001, ****$p$< 0.0001, ns $p \geq 0.05$.


https://doi.org/10.2147/JIR.S500115

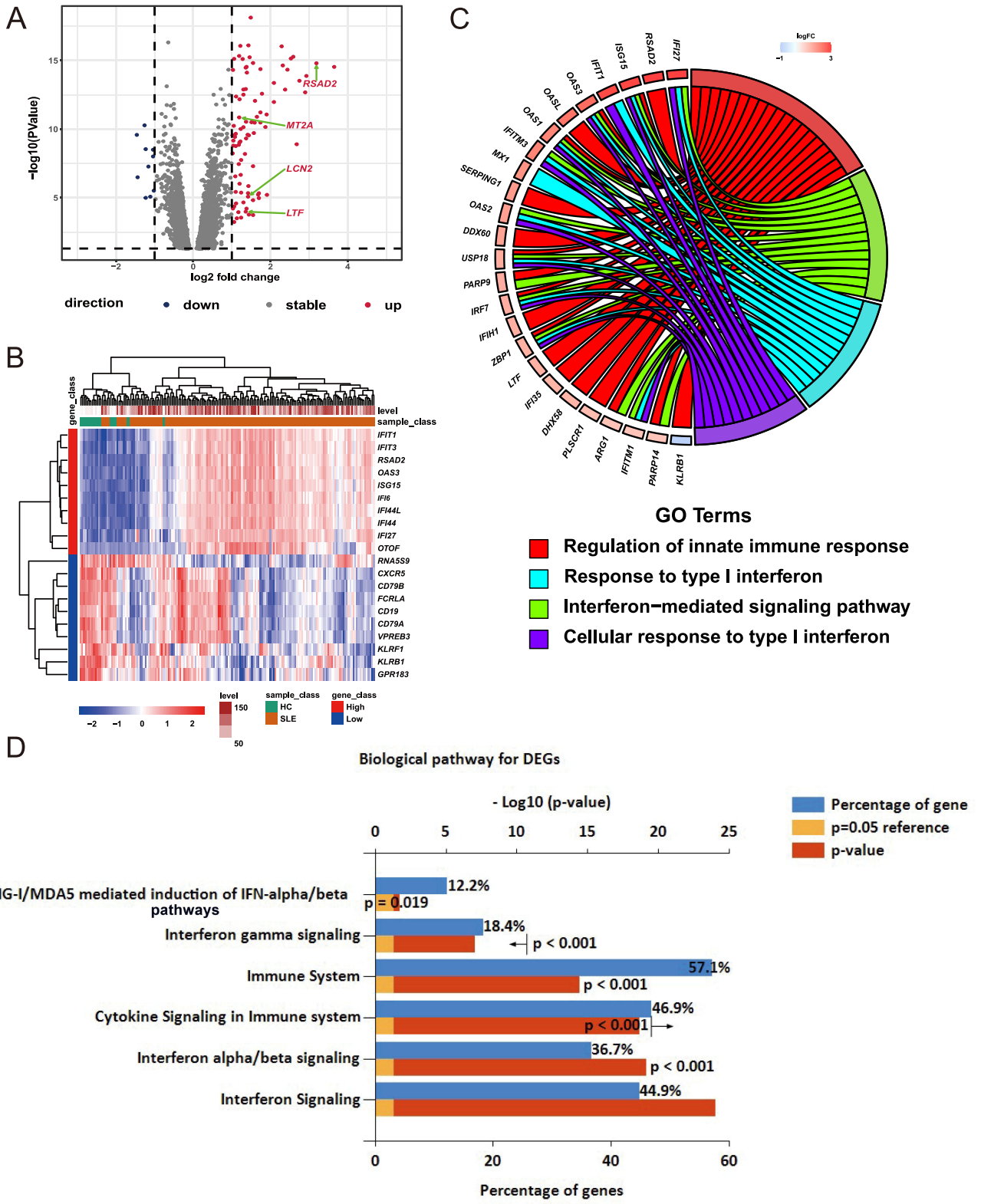


**Figure 2** Identification and biological enrichment analyses of genes from GSE72326. (**A**) Volcano plot illustrating the distribution of DEGs in GSE72326. Nodes in red represent up-regulated genes, blue represent down-regulated genes, and gray represent no significantly changed genes (|log2 FC |> 1, $p < 0.05$). (**B**) The heatmap of top 20 DEGs in GSE72326. Blue and red colors represent low and high expression values, respectively. (**C**) 4950 Dataset genes in SLE for GO enrichment. (**D**) KEGG enrichment analysis of 4950 dataset genes involved in SLE progression. Top 6 terms of KEGG analysis in biological pathway category (ranked by *p*-value).

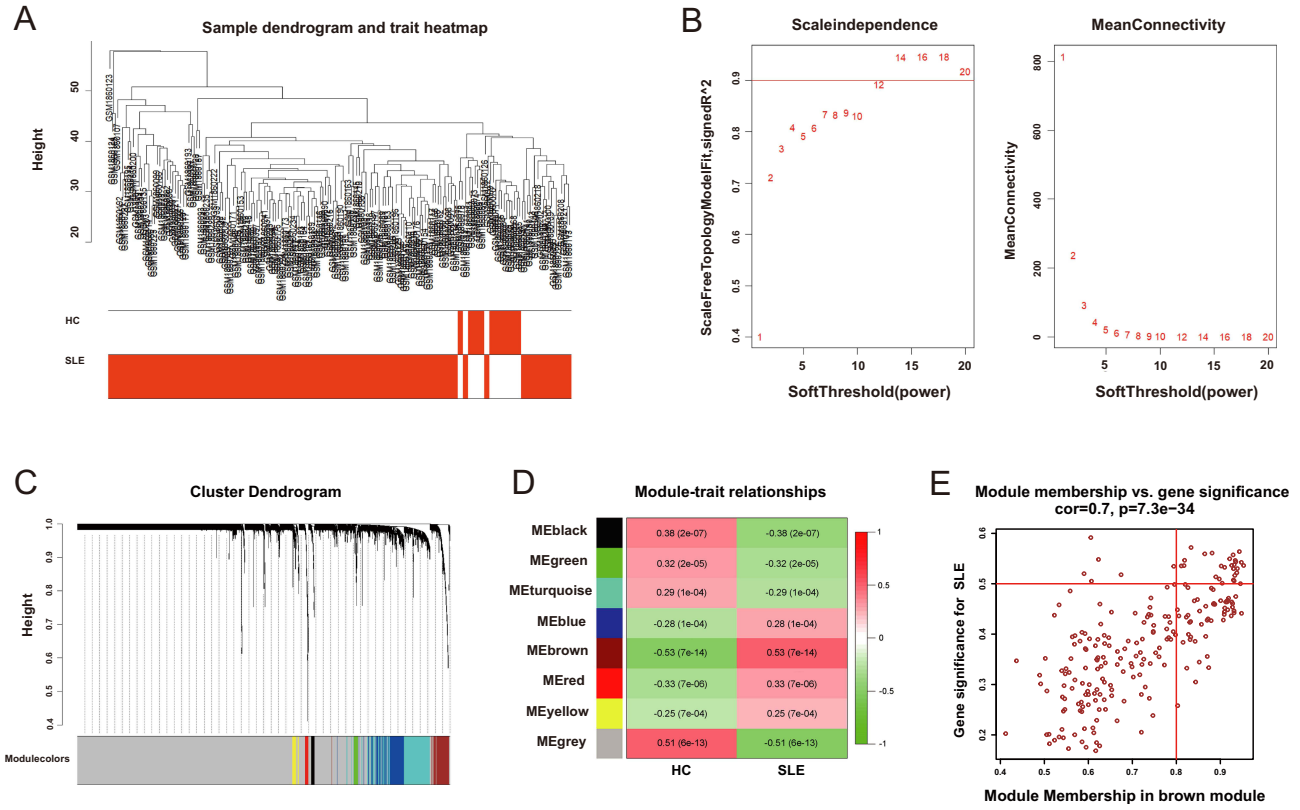


**Figure 3** Construction of WGCNA in GSE72326 dataset. (**A**) Clustering dendrogram of samples. (**B**) Network topology analysis of different soft-threshold power. The left panel displayed the impact of soft-threshold power on scale-free topology fit index. The right panel showed the impact of soft-threshold power on the mean connectivity. (**C**) The cluster dendrogram of all genes in GSE72326 dataset based on different metric clustering (1-TOM). Branches of the cluster dendrogram were classified to 8 color-coded modules when threshold for the merge of similar modules was defined as 0.25. Each branch represents a gene, and the color of each module represents a co-expression module. (**D**) The module-trait heatmap of the correlation between gene clustering modules and the progress of SLE in GSE72326 dataset. Each color represents one co-expression module. *RSAD2* in the module of chiefly enriched in correlated with the occurrence of SLE. (**E**) The scatter diagram of the module with the most positive correlation in GSE72326 dataset.

yellow). This yielded 4 hub IM-DEGs: *RSAD2, MT2A, LCN2*, and *LTF*, which are likely key regulators of iron metabolism in SLE (Figure 4D). These genes may serve as potential biomarkers or therapeutic targets for SLE, highlighting the pivotal role of iron dysregulation in its pathogenesis.

## Verification of the IM-Related Biomarkers for SLE Diagnosis

To investigate whether the 4 identified IM-DEG biomarkers could serve as novel clinical diagnostic indicators for SLE and RA, a validation was conducted using the dataset GSE110169 dataset.[22] This dataset includes samples from 77 healthy individuals, 82 SLE patients, and 84 RA patients. The analysis focused on the development of a risk prediction model, which demonstrated promising performance, as evidenced by the calibration curve that showed strong agreement between predicted and actual disease probabilities (Figure 5A). This underscores the robustness of the model in predicting SLE risk with minimal deviation, as seen by the consistency of the apparent, bias-corrected, and ideal curves. A nomogram was constructed to further elucidate the contribution of 4 IM-DEGs (*MT2A, LCN2, LTF* and *RSAD2*) to SLE risk prediction. *RSAD2*, in particular, emerged as the most significant contributor. The combined predictive score from these variables allowed for an accurate estimation of individual SLE risk (Figure 5B).

To assess the diagnostic capabilities of the biomarkers, ROC curves were generated. Among the 4 IM-DEGs, *RSAD2* exhibited the highest diagnostic value for SLE, with an AUC of 0.927 (Figure 5C), suggesting its potential as a highly reliable biomarker for SLE diagnosis. In contrast, *MT2A, LCN2*, and *LTF* demonstrated moderate to lower AUC values, indicating relatively weaker predictive power. To explore the discriminative ability of these biomarkers in differentiating SLE from RA, a second ROC analysis was performed. *RSAD2* once again showed the highest diagnostic accuracy,


https://doi.org/10.2147/JIR.S500115

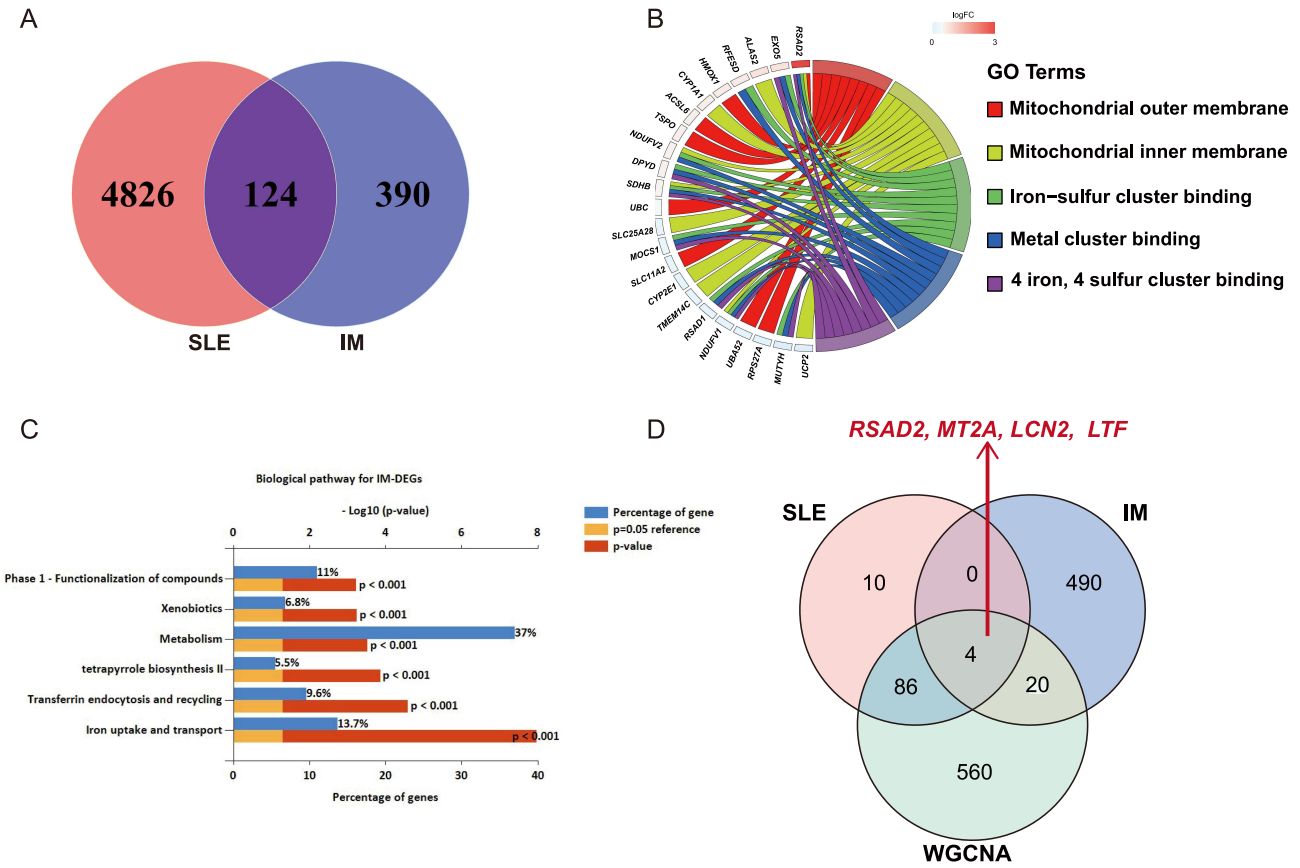


**Figure 4** Overlapping dataset genes in SLE and IM-related genes and related enrichment analyses. (**A**) Venn diagram of overlapping dataset genes ($p < 0.05$) in SLE and iron metabolism-related genes. (**B**) GO term enrichment analysis of 124 IM-Genes. (**C**) KEGG enrichment analysis of genes involved in iron metabolism. Top 6 terms of KEGG analysis in biological pathway category (ranked by $p$ value). (**D**) Venn diagram of overlapping between 100 DEGs in SLE, iron metabolism related genes and genes from high correlation within the modules in WGCNA.

achieving an AUC of 0.909 (Figure 5D). This finding highlights *RSAD2*'s capacity not only to diagnose SLE but also distinguish it from RA, two autoimmune diseases that share clinical similarities. In summary, *RSAD2* consistently demonstrated superior diagnostic performance, with AUC values exceeding 0.9 in both SLE diagnosis and differentiation from RA. These findings suggest that *RSAD2* could be a reliable biomarker for predicting occurrence of SLE and could potentially serve as a valuable tool in evaluating therapeutic efficacy in clinical settings.

## Identification of RSAD2 as a Key Biomarker in SLE-Associated Iron Metabolism

The 124 IM-Genes were subsequently subjected to LASSO regression algorithm to pinpoint high-value diagnostic biomarkers. The LASSO model generated a coefficient profile (Figure 6A), indicating how the variables were progressively regularized. Following cross-validation (Figure 6B), 20 candidate biomarkers were retained, based on the optimized log λ value, which minimized the error rate. Subsequently, these 20 genes were compared against the set of significant IM-DEGs, and their intersection revealed *RSAD2* as a uniquely shared biomarker (Figure 6C).

## Validation of RSAD2 Expression in SLE

To validate the differential expression of *RSAD2*, we further analyzed two independent public datasets (GSE50772, and GSE126307), alongside clinical blood samples. Consistent with our previous results, *RSAD2* was significantly upregulated in SLE group compared to HCs, as demonstrated in both datasets (Figure 7A and B). To further corroborate these findings, we collected fresh peripheral blood from a cohort comprising 20 hCs and 46 SLE patients (Table 2). RT-qPCR analysis revealed a significant increase in *RSAD2* transcription in the SLE patients (Figure 7C, $p = 0.004$), reinforcing the results observed in the independent datasets. Furthermore, we assessed the protein expression of viperin, encoded by

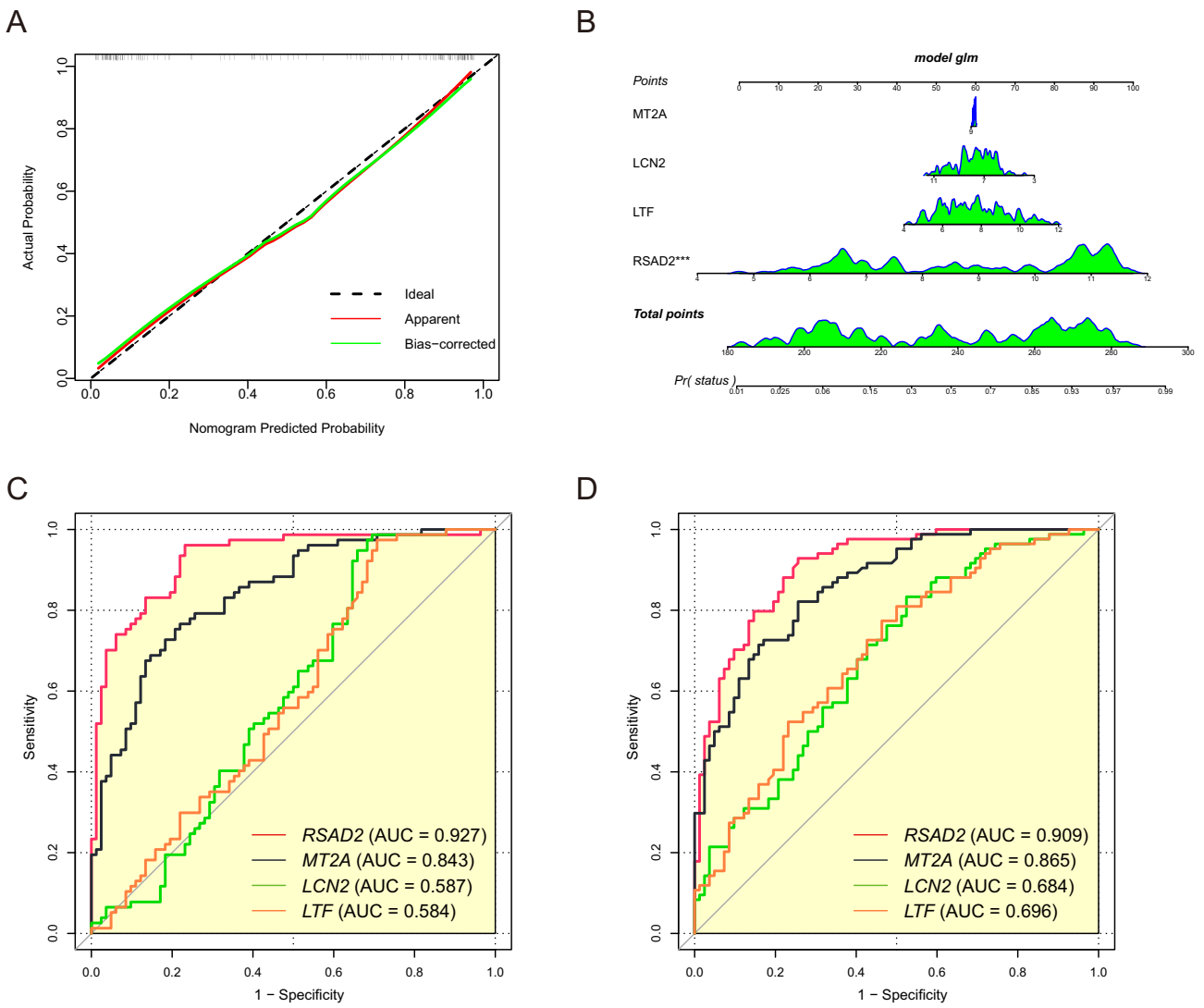


**Figure 5** Diagnose significance of *RSAD2* in SLE. (**A** and **B**) Calibration curve (**A**) and Nomogram (**B**) estimates SLE risk by locating points corresponding to the expression levels of *MT2A*, *LCN2*, *LTF* and *RSAD2* genes, summing these points to calculate a total score, and then determining the estimated risk on the bottom axis. (**C**) ROC curves for evaluating potential diagnostic value of *RSAD2* in SLE patients. (**D**) ROC curves for evaluating the possibility and effect of *RSAD2* to identify RA from SLE. The red curve represents *RSAD2*, the black curve represents *MT2A*, the green curve represents *LCN2*, the Orange curve represents *LTF*. ***$p < 0.001$.

*RSAD2*, using Western blot analysis. The data demonstrated a significant upregulation of viperin in SLE patients compared to HCs, with a marked increase in the viperin/GAPDH ratio ($p = 0.0083$) (Figure 7D).

## Correlation Analysis of Classic SLE Biomarkers and RSAD2 Expression

Several traditional molecular biomarkers assist in diagnosing SLE by reflecting disease activity and organ involvement through their serum concentrations. In this study, we analyzed the correlation between key biomarkers, including albumin, blood urea nitrogen (BUN), creatinine, complement components C3, and C4, as well as IgG, with the expression levels of *RSAD2*. Our results indicate significant associations between these biomarkers and *RSAD2* expression, which may provide further insight into the molecular mechanisms underlying SLE pathogenesis (Figure 8A–F). Albumin exhibited a moderate positive correlation with *RSAD2* expression (r = 0.3499, $p = 0.0171$), suggesting that reduced serum albumin levels, often observed in SLE patients with nephritis, may coincide with lower *RSAD2* expression (Figure 8A). BUN and creatinine, both markers of renal function, also showed moderate to strong positive correlations (r = 0.411, $p = 0.0055$; r = 0.4784, $p = 0.0010$, respectively) (Figures 8B and C). This suggests that increased *RSAD2* expression may drive impaired renal function, a common feature in LN. Conversely, C3 and C4 were negatively correlated with *RSAD2* expression (r = −0.4735, $p$ =


https://doi.org/10.2147/JIR.S500115

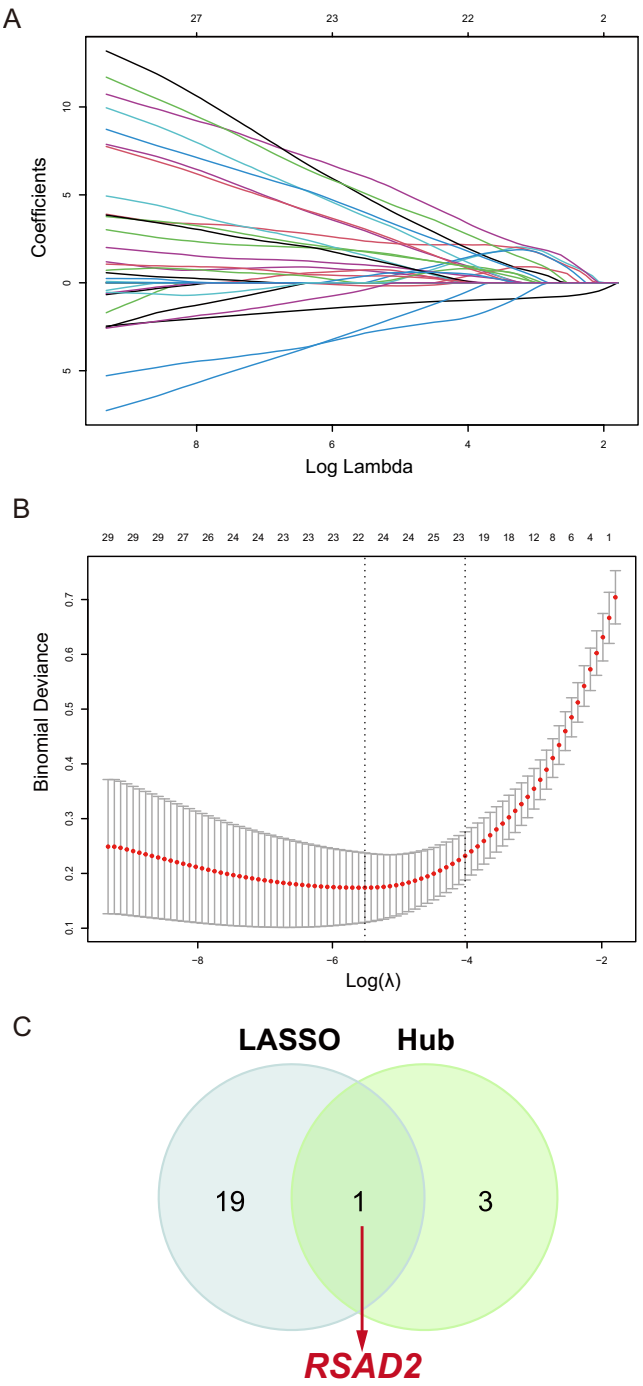


**Figure 6** Results of the key biomarker related to IM in SLE. (**A**) Results of LASSO regression model. (**B**) The chart illustrates the LASSO model's regularisation path, with binomial deviance on the y-axis and log (λ) on the x-axis, indicating model fit and complexity with varying λ. Red dots and error bars reflect deviance and non-zero coefficient counts for IM-Genes. (**C**) Venn diagram showing the overlap between 4 important IM-DEGs and results of LASSO.

0.0054; r = −0.3809, $p$ = 0.0287, respectively) (Figure 8D and E). This aligns with the clinical observation that decreased complement levels, associated with active SLE disease and immune complex formation, may be inversely related to *RSAD2* expression. Finally, IgG levels demonstrated a strong positive correlation with *RSAD2* expression (r = 0.5636, $p$ = 0.0012) (Figure 8F), reinforcing the potential role of *RSAD2* in the heightened immune activation observed in SLE. These findings highlight *RSAD2* as a promising biomarker, potentially reflective of both immune activation and renal involvement in SLE, and warrant further investigation into its mechanistic role in lupus pathogenesis.

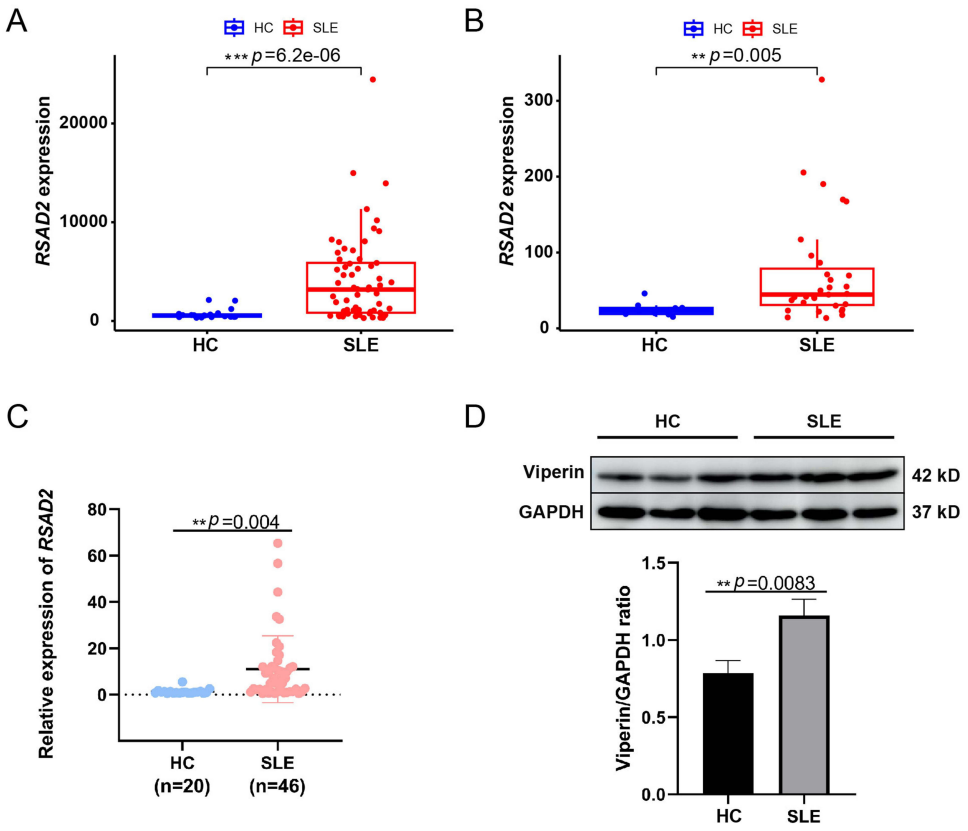


**Figure 7** Verifying the expression of *RSAD2*. (**A** and **B**) GSE50772 (**A**) and GSE126307 (**B**) datasets were used to validate the expression of *RSAD2*. (**C**) RT-qPCR determination of expression of *RSAD2* mRNA in SLE patients (n = 46) compared with HCs (n = 20). (**D**) Western blot analysis of the expression of viperin in PBMCs of HCs and patients with SLE and the protein expression level is calculated by the ratio of protein to GAPDH (n = 3). All experiments are conducted in triplicate. Data were presented with mean ± SD. $^{**}p < 0.01$, $^{***}p < 0.001$.

## Immune Infiltration Evaluation and Correlation Analysis Between Genes and Immune Cells

Based on our findings, *RSAD2* has emerged as a significant IM-DEG in SLE and holds potential as a key regulator in immune modulation and iron metabolism. Moreover, immune cells, particularly DCs, macrophages and neutrophils, have been implicated in kidney infiltration LN, potentially exacerbating renal pathology. To further investigate immune cell infiltration, we utilized CIBERSORT deconvolution algorithms to quantify the proportions of 22 immune cell types in SLE and healthy groups. The box plot analysis revealed significant infiltration differences between these groups. Specifically, monocytes ($p < 0.0001$) and activated DCs ($p < 0.001$) demonstrated higher infiltration in the SLE cohort. In contrast, naïve B cells ($p < 0.01$) and CD4 memory resting T cells ($p < 0.0001$) exhibited reduced infiltration in SLE compared to controls (Figure 9A). Despite these immune cell distribution changes, the correlation analysis *RSAD2* expression and naïve B cells, monocytes or CD4 memory resting T cells revealed weak associations (Figure 9B–D). Intriguingly, a positive correlation between *RSAD2* expression and activated DCs infiltration was observed (R = 0.39, $p = 3.1e-07$; Figure 9E), suggesting a more prominent role for *RSAD2* in DC-mediated immune responses. Furthermore, a heatmap analysis depicting correlations between 4 IM-DEGs and 21 immune cell types highlighted *RSAD2*'s pronounced association with activated DCs, further supporting its relevance in shaping the immune microenvironment in SLE. Among the examined genes, *RSAD2* exhibited the strongest correlation with activated DCs, implying that it might play a pivotal role in monocyte-to-DC differentiation and contribute to the pathogenesis of SLE, potentially via mechanisms involving iron metabolism (Figure 9F).


https://doi.org/10.2147/JIR.S500115

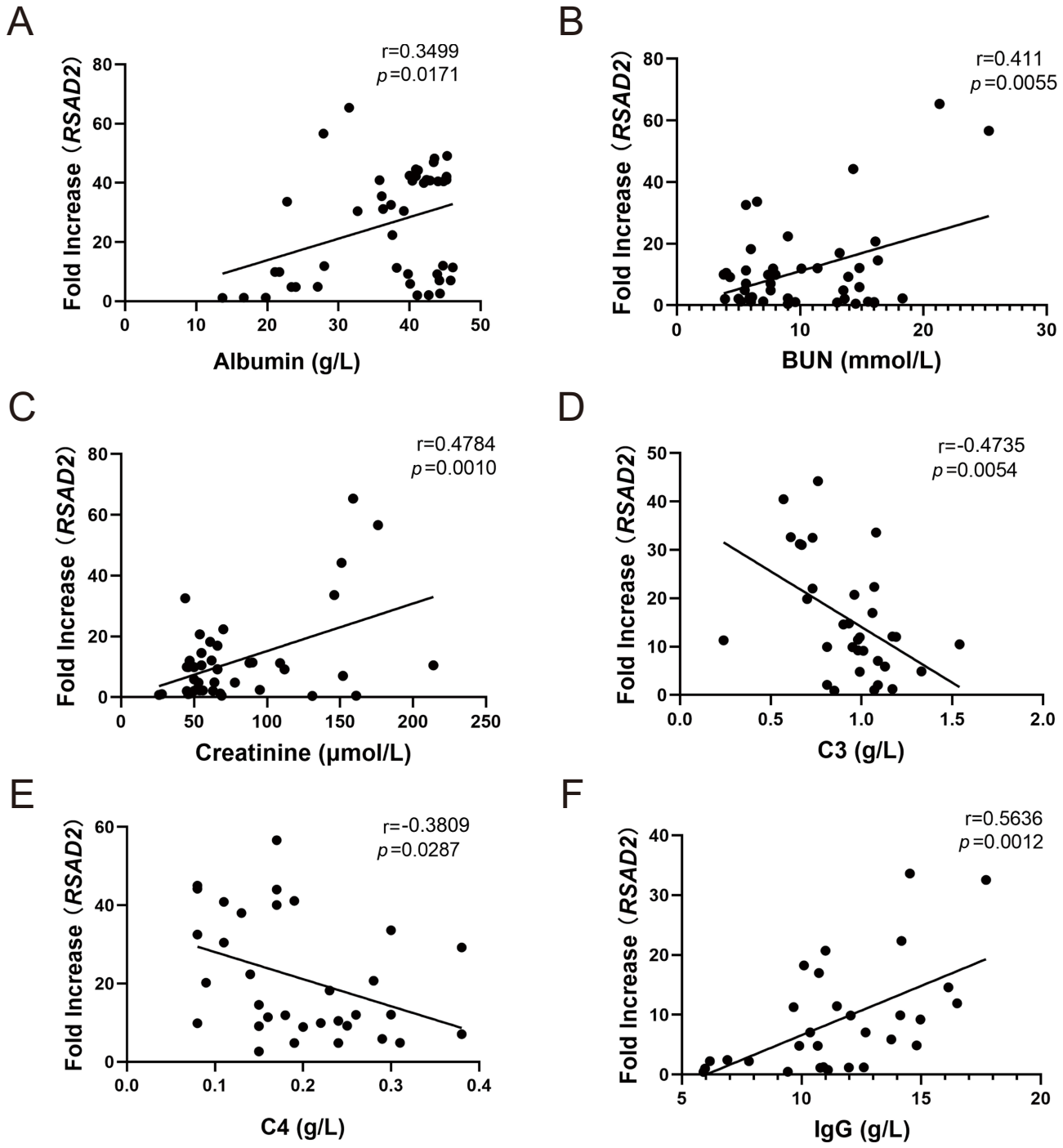


**Figure 8** Correlation analysis between classic clinical biomarkers of SLE and the expression level of *RSAD2*. (**A-F**) Correlation between *RSAD2* and commonly used diagnostic indicators (albumin, BUN, creatinine, C3, C4, and IgG) in clinical practice.

## Knockdown of Rsad2 in Activated DCs Affects the Expression of Inflammatory Mediators and Iron Metabolism Genes

Immune infiltration analysis revealed a strong association between activated DCs and *RSAD2* expression in patients with SLE. To investigate the functional role of *Rsad2* in DC activation, we cultured bone marrow-derived DCs in vitro and treated them with LPS or LPS in combination with TREM-1 agonists, a combination known to enhance DC activation. *Rsad2* expression was markedly elevated in activated DCs, particularly with the combination of LPS and TREM-1 agonists, highlighting its

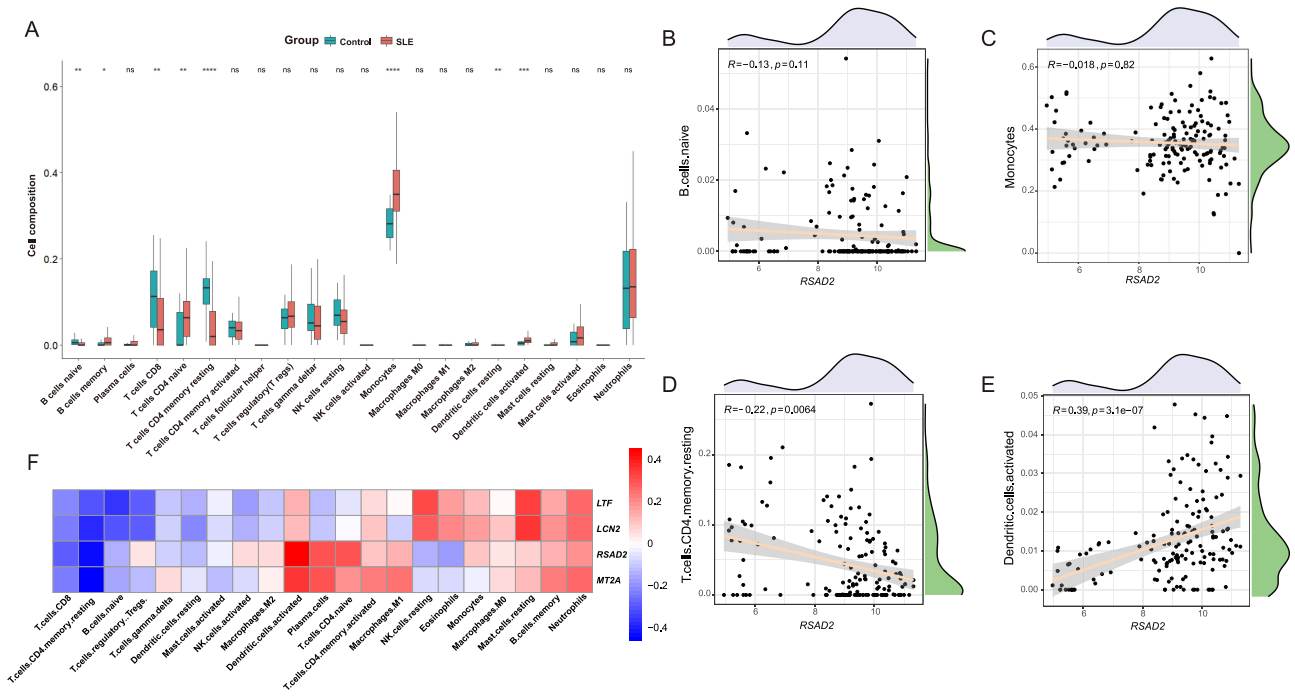


**Figure 9** Evaluation of immune cell infiltration and immune correlation analysis. (**A**) Box diagram of the proportion of 22 types of immune cells in GSE72326 with SLE group versus HC group. *$p$ < 0.05, **$p$ < 0.01, ***$p$ < 0.001, ****$p$< 0.0001, ns $p$ ≥ 0.05. (**B-E**) Correlation scatter diagram of expression of *RSAD2* with, CD4 memory resting T cells (R = −0.22, $p$ = 0.0064) and activated DCs (R = 0.39, $p$ = 3.1e-07) infiltration level. (**F**) Heatmap of correlations between IM-DEGs (*RSAD2, LTF, MT2A*, and *LCN2*) and infiltrating immune cells. Darker color implies stronger association.

association with activation states of DCs (Figure 10A). To further explore the role of *Rsad2*, we performed RNA interference to knock down its expression, as validated by RT-qPCR and Western blot (Figure 10B and C). The silencing of *Rsad2* significantly suppressed the production of key inflammatory cytokines, including IL-6, TNF-α, and MCP-1 (Figure 10D–F), underscoring its role in regulating the inflammatory response in DCs. This reduction in inflammatory mediators suggests that *Rsad2* plays a pivotal role in modulating immune responses during DC activation. Additionally, given that *Rsad2* has been identified as a key regulator of iron metabolism, we assessed the expression of classic iron metabolism related genes following *Rsad2* knockdown. Interestingly, *Hamp* and *Fth1*, two critical regulators of iron sequestration and storage were significantly upregulated. Meanwhile, due to the silence of *RSAD2, Slc40a*, a gene encoding ferroprotein was also upregulated (Figure 10G–I). These findings suggest that *Rsad2* in not only crucial for inflammatory responses but also plays a significant role in the regulation of iron metabolism in activated DCs.

## Discussion

In this study, we employed bioinformatics analyses to identify 124 IM-Genes between SLE patients and HCs using gene expression profiles from GSE72326 and the MSigDB database. GO and KEGG analyses revealed that these IM-Genes are significantly associated with metal ion metabolism and the IFN signaling pathway, which is crucial in SLE pathogenesis. Subsequently, WGCNA was utilized to identify hub genes among the IM-Genes, with 4 IM-DEGs (*RSAD2, LTF, LCN2*, and *MT2A*) emerging as particularly noteworthy due to their significant expression characteristics in the clinical significance module and close association with iron metabolism.

Our findings demonstrate a correlation between *RSAD2* expression levels and clinical indicators of SLE. We utilized machine learning techniques and the validation set GSE110169 to develop and evaluate a clinical prediction model. Consistent with our bioinformatics analyses, *RSAD2* expression was confirmed to be significantly elevated in PBMCs of SLE patients. Among the 4 common IM-DEGs identified, *RSAD2* exhibited the highest sensitivity and specificity in distinguishing SLE patients from both healthy individuals and RA patients. These data suggest that *RSAD2* may play a crucial role in SLE pathogenesis and could serve as a specific biomarker for diagnosing iron metabolism disorders in SLE patients, potentially facilitating more precise treatment strategies.


https://doi.org/10.2147/JIR.S500115

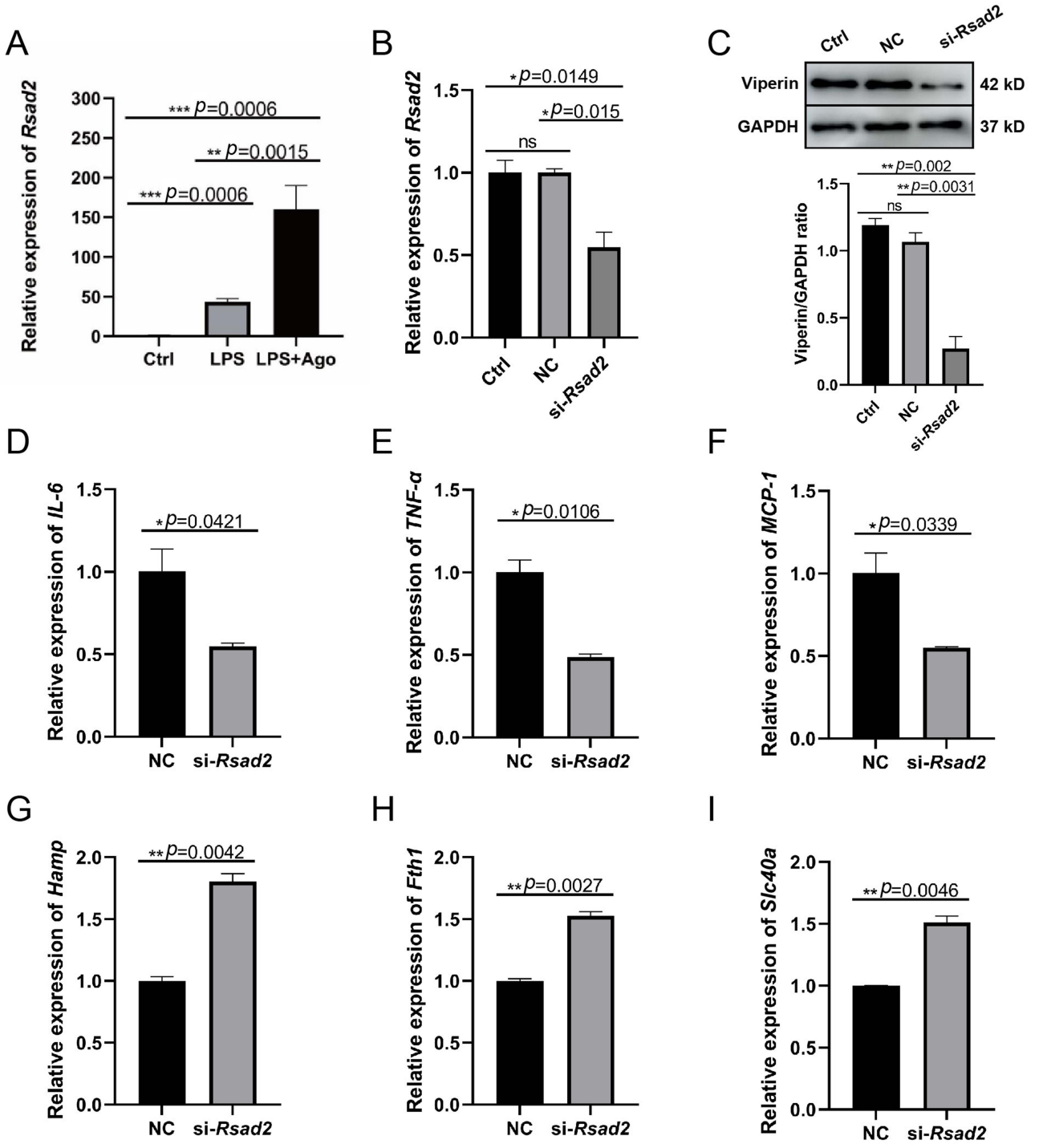


**Figure 10** Knockdown of *Rsad2* in murine DCs inhibited their overactivation and regulated iron metabolism genes expression. (**A**) RT-qPCR determination of *Rsad2* mRNA expression in LPS or LPS in combination with TREM-1 agonists activated DCs. (**B** and **C**) Activated DCs were transfected with small interfering RNA or negative control (NC), and the expressions of *Rsad2* and viperin were measured by RT-qPCR (**B**) and Western blot (**C**). (**D**–**F**) The expressions of IL-6 (**D**), TNF-α (**E**), and MCP-1 (**F**) were determined by RT-qPCR. (**G**–**I**) The expressions of *Hamp* (**G**), *Fth1* (**H**), and *Slc40a* (**I**) were detected by RT-qPCR. All of the experiments were performed in triplicate. Data were presented with means ± SD. *$p < 0.05$, **$p < 0.01$, ***$p < 0.001$.

*RSAD2*, a key ISG, plays a pivotal role in activating the immune response and has been implicated in multiple autoimmune diseases.[23] Previous studies have established a significant association between SLE patients and dysregulation of IFN and expression of ISGs. In cross-sectional SLE studies, the IFN signature has been demonstrated to correlate with disease activity. Five ISGs (*NRIR, RSAD2, USP18, IFI44*, and *ISG15*) have been identified as biomarkers for the

diagnosis and stratification of SLE.[24] A meta-analysis revealed that *RSAD2* is a hub gene of the SLE-associated "magenta" module and is significantly upregulated in SLE patients compared to normal controls.[23] However, it is worth noting that currently, IFN-α levels are challenging to measure, and the ISG signature is not yet available in clinical routine.[25] A systematic review revealed that the expression of ISGs used for the IFN signature in SLE patients was influenced more by ancestry than disease activity.[26] Therefore, further exploration is urgently needed to elucidate more precise regulatory mechanisms regarding IFN-related genes.

In SLE patients, *RSAD2* is highly expressed in various $CD4^+$ T-cell subsets, potentially promoting B-cell activation by fostering the differentiation of T helper 17 (Th17) and T follicular helper (Tfh) cells.[27] A previous study indicated that *RSAD2* is required for IRF7-mediated type I IFNs secretion by myeloid DCs (mDCs).[28] Our results align with the findings, suggesting that *RSAD2* not only participates in IFN-related pathways but also closely correlates with activated DCs in the immune infiltration of SLE. Intriguingly, our in vitro experiments demonstrated that activated DCs express higher level of *Rsad2*, while knockdown of *Rsad2* significantly inhibited the inflammatory cytokines produced by activated DCs, highlighting the important role of *Rsad2* in the regulating immune function in DCs.

In this study, we have elucidated the novel relationship between *RSAD2* and iron metabolism within the context of SLE, supported by an integration of clinical data and bioinformatics analyses. Previous studies have indicated that disruptions of iron metabolism can influence SLE by impairing the function and metabolism of specific immune cells, such as T cells.[29] Furthermore, research has highlighted potential pathways where iron accumulation, oxidative stress, and lipid peroxidation contribute to ferroptosis, a recognized aspect of SLE pathogenesis.[30] Viperin, encoded by *RSAD2*, features a radical S-adenosylmethionine (RS) enzyme domain and a [4Fe-4S] cluster, playing a crucial role in biological processes with a primary focus on antiviral activity.[27] Our RNAi data reveal that knockdown of *Rsad2* significantly impacts the expression of key iron metabolism genes (*Hamp, Fth1*, and *Slc40a*) in activated DCs. Based on our findings, it is crucial to investigate the implications of the observed relationship between *Rsad2* and iron metabolism in the context of SLE. The modulation of iron metabolism by *Rsad2* in activated DCs may represent a pivotal mechanism underlying immune dysregulation in SLE. Specifically, *Rsad2* may influence vital genes involved in iron metabolism, such as *Hamp* and *Fth1*, with ferritin primarily serving to store iron in a soluble and non-toxic form, potentially leading to abnormal iron storage. Additionally, *Rsad2* may inhibit the expression of *Slc40a*, a gene implicated in iron export, resulting in the abnormal accumulation of intracellular iron and subsequent imbalance in iron metabolism. This imbalance could exacerbate oxidative stress and promote the inflammatory responses characteristic of SLE. Furthermore, the interplay between *Rsad2*-mediated iron metabolism warrants further investigation, as it may reveal novel therapeutic targets aimed at mitigating the pathogenic processes in SLE.

Despite these insights, our study has several limitations that warrant further investigation. While we have demonstrated the involvement of *RSAD2*, the precise molecular mechanisms by which it influences SLE pathogenesis and progression remain to be fully elucidated. Our experimental scope was primarily focused on examining *Rsad2*'s effects on inflammatory cytokines production and iron metabolism-related gene expression in murine bone marrow-derived DCs. However, the detailed molecular pathways through which *Rsad2* orchestrates iron homeostasis in DCs require further clarification. Moreover, the intricate relationship between *Rsad2*-mediated regulation of iron metabolism and its impact on DC activation states needs to be comprehensively explored in future studies.

## Conclusion

In summary, our research has unveiled the significant role of *RSAD2* in SLE pathogenesis and its potential as a dual-purpose biomarker for diagnosing iron metabolism imbalances and immune dysregulation in SLE patients. The diagnostic capabilities of *RSAD2* were confirmed, and its involvement in SLE pathogenesis was clarified through the application machine learning techniques. Notably, *RSAD2* is linked to pathways governing iron metabolism and IFN signaling, shedding light on the molecular underpinnings of SLE. Our findings also underscore the role of dysregulated DCs in SLE, suggesting avenues for immune-modulatory treatments. The discovery of *RSAD2*'s influence on the immune responses of DCs via the iron metabolism pathway opens new possibilities for investigating and managing SLE. Collectively, this study enhances our understanding of SLE pathogenesis and paves the way for refined diagnostic tools and dual-targeted therapeutic strategies.

## Data Sharing Statement

The data supporting the conclusions of this article are available in the article, Supplementary material, and the GEO repository (https://www.ncbi.nlm.nih.gov/geo/), MSigDB (http://software.broadinstitute.org/gsea/index.jsp), DAVID database (https://david.ncifcrf.gov). Further inquiries can be directed to the corresponding authors. The "Key resources table" section indicated all analyses methods, software packages, and online tools. Code requirements can be directed to the corresponding authors.

## Ethics Approval and Informed Consent

This study was conducted in accordance with the Declaration of Helsinki and approved by the Clinical Research Ethics Committee of the First Affiliated Hospital of Wenzhou Medical University, and all participants have signed consent forms. The Issuing Number is KY2023-083. All experiments using mice were approved by the Institutional Animal Care and Use Committee at Wenzhou Medical University (Animal Welfare Assurance), the approval number for animal ethics is xmsq2022-0792 and complied with the National Institutes of Health Guide for the Care and Use of Laboratory Animals.

## Consent for Publication

All authors have read the manuscript in its entirety and agree to its publication with currently content.

## Acknowledgments

This study was a re-analysis based on published data from the GEO database and MSigDB databases. We would like to thank these databases for sharing the data.

## Author Contributions

All authors made a significant contribution to the work reported, whether that is in the conception, study design, execution, acquisition of data, analysis and interpretation, or in all these areas; have drafted or written, or substantially revised or critically reviewed the article; have agreed on the journal to which the article will be submitted; reviewed and agreed on all versions of the article before submission, during revision, the final version accepted for publication, and any significant changes introduced at the proofing stage; agree to take responsibility and be accountable for the contents of the article.

## Funding

This study was supported by National innovation and Entrepreneurship Training Program for College Students [grant number 202310343026]; Zhejiang College Students Innovative Entrepreneurial Training Program (New Young Talent Program) [grant number 2023R413022]; the Natural Science Foundation of Zhejiang Province [grant number LTGY23H100001]; Science and Technology Plan Project of Wenzhou Municipality, China [grant numbers. Y20220389, Y20220045]; and Major Science & Technology Innovation Project of Wenzhou, China [grant number ZY2022017].

## Disclosure

The authors declare no competing interests.

## References

1. Ceccarelli F, Perricone C, Natalucci F, et al. Organ damage in systemic lupus erythematosus patients: a multifactorial phenomenon. *Autoimmun Rev*. 2023;22:103374. doi:10.1016/j.autrev.2023.103374
2. Gualtierotti R, Biggioggero M, Penatti AE, Meroni PL. Updating on the pathogenesis of systemic lupus erythematosus. *Autoimmun Rev*. 2010;10:3–7. doi:10.1016/j.autrev.2010.09.007
3. Hong Y, Wang D, Lin Y, et al. Environmental triggers and future risk of developing autoimmune diseases: molecular mechanism and network toxicology analysis of bisphenol A. *Ecotoxicol Environ Saf*. 2024;288:117352. doi:10.1016/j.ecoenv.2024.117352
4. Psarras A, Emery P, Vital EM. Type I interferon-mediated autoimmune diseases: pathogenesis, diagnosis and targeted therapy. *Rheumatology*. 2017;56:1662–1675. doi:10.1093/rheumatology/kew431

5. Liu J, Zhang X, Cao X. Dendritic cells in systemic lupus erythematosus: from pathogenesis to therapeutic applications. *J Autoimmun*. 2022;132:102856. doi:10.1016/j.jaut.2022.102856
6. Wang F, Lv H, Zhao B, et al. Iron and leukemia: new insights for future treatments. *J Exp Clin Cancer Res*. 2019;38:406. doi:10.1186/s13046-019-1397-3
7. Voulgarelis M, Kokori SI, Ioannidis JP, Tzioufas AG, Kyriaki D, Moutsopoulos HM. Anaemia in systemic lupus erythematosus: aetiological profile and the role of erythropoietin. *Ann Rheum Dis*. 2000;59:217–222. doi:10.1136/ard.59.3.217
8. Scindia Y, Wlazlo E, Ghias E, et al. Modulation of iron homeostasis with hepcidin ameliorates spontaneous murine lupus nephritis. *Kidney Int*. 2020;98:100–115. doi:10.1016/j.kint.2020.01.025
9. Li P, Jiang M, Li K, et al. Glutathione peroxidase 4-regulated neutrophil ferroptosis induces systemic autoimmunity. *Nat Immunol*. 2021;22:1107–1117. doi:10.1038/s41590-021-00993-3
10. Ohl K, Rauen T, Tenbrock K. Dysregulated neutrophilic cell death in SLE: a spotlight on ferroptosis. *Signal Transduct Target Ther*. 2021;6:392. doi:10.1038/s41392-021-00804-z
11. Wang Z, Monteiro CD, Jagodnik KM, et al. Extraction and analysis of signatures from the gene expression omnibus by the crowd. *Nat Commun*. 2016;7:12846. doi:10.1038/ncomms12846
12. Hong Y, Yuan Q, Wang L, et al. Integrative bioinformatics analysis to identify ferroptosis-related genes in non-obstructive azoospermia. *J Assist Reprod Genet*. 2024;41:2145–2161. doi:10.1007/s10815-024-03155-0
13. Shen H, Wu H, Sun F, Qi J, Zhu Q. A novel four-gene of iron metabolism-related and methylated for prognosis prediction of hepatocellular carcinoma. *Bioengineered*. 2021;12:240–251. doi:10.1080/21655979.2020.1866303
14. Chen T, Zhang H, Liu Y, Liu YX, Huang L. EVenn: easy to create repeatable and editable venn diagrams and venn networks online. *J Genet Genomics*. 2021;48:863–866. doi:10.1016/j.jgg.2021.07.007
15. Zhu J, Lu Q, Liang T, et al. Development and validation of a machine learning-based nomogram for prediction of ankylosing spondylitis. *Rheumatol Ther*. 2022;9:1377–1397. doi:10.1007/s40744-022-00481-6
16. Robin X, Turck N, Hainard A, et al. pROC: an open-source package for R and S+ to analyze and compare ROC curves. *BMC Bioinf*. 2011;12:77. doi:10.1186/1471-2105-12-77
17. Iasonos A, Schrag D, Raj GV, Panageas KS. How to build and interpret a nomogram for cancer prognosis. *J Clin Oncol*. 2008;26:1364–1370. doi:10.1200/jco.2007.12.9791
18. Newman AM, Liu CL, Green MR, et al. Robust enumeration of cell subsets from tissue expression profiles. *Nat Methods*. 2015;12:453–457. doi:10.1038/nmeth.3337
19. Hochberg MC. Updating the American College of Rheumatology revised criteria for the classification of systemic lupus erythematosus. *Arthritis Rheum*. 1997;40:1725. doi:10.1002/art.1780400928
20. Gladman DD, Ibañez D, Urowitz MB. Systemic lupus erythematosus disease activity index 2000. *J Rheumatol*. 2002;29:288–291.
21. Chiche L, Jourde-Chiche N, Whalen E, et al. Modular transcriptional repertoire analyses of adults with systemic lupus erythematosus reveal distinct type I and type II interferon signatures. *Arthritis Rheumatol*. 2014;66:1583–1595. doi:10.1002/art.38628
22. Hu Y, Carman JA, Holloway D, et al. Development of a molecular signature to monitor pharmacodynamic responses mediated by in vivo administration of glucocorticoids. *Arthritis Rheumatol*. 2018;70:1331–1342. doi:10.1002/art.40476
23. Sezin T, Vorobyev A, Sadik CD, Zillikens D, Gupta Y, Ludwig RJ. Gene expression analysis reveals novel shared gene signatures and candidate molecular mechanisms between pemphigus and systemic lupus erythematosus in CD4(+) T cells. *Front Immunol*. 2017;8:1992. doi:10.3389/fimmu.2017.01992
24. Shen M, Duan C, Xie C, et al. Identification of key interferon-stimulated genes for indicating the condition of patients with systemic lupus erythematosus. *Front Immunol*. 2022;13:962393. doi:10.3389/fimmu.2022.962393
25. Enocsson H, Wetterö J, Eloranta ML, et al. Comparison of surrogate markers of the type I interferon response and their ability to mirror disease activity in systemic lupus erythematosus. *Front Immunol*. 2021;12:688753. doi:10.3389/fimmu.2021.688753
26. Siddiqi KZ, Wilhelm TR, Ulff-Møller CJ, Jacobsen S. Cluster of highly expressed interferon-stimulated genes associate more with African ancestry than disease activity in patients with systemic lupus erythematosus. A systematic review of cross-sectional studies. *Transl Res*. 2021;238:63–75. doi:10.1016/j.trsl.2021.07.006
27. Xin Y, He Z, Mei Y, et al. Interferon-α regulates abnormally increased expression of RSAD2 in Th17 and Tfh cells in systemic lupus erythematosus patients. *Eur J Immunol*. 2023;53:e2350420. doi:10.1002/eji.202350420
28. Jang JS, Lee JH, Jung NC, et al. Rsad2 is necessary for mouse dendritic cell maturation via the IRF7-mediated signaling pathway. *Cell Death Dis*. 2018;9:823. doi:10.1038/s41419-018-0889-y
29. Voss K, Sewell AE, Krystofiak ES, et al. Elevated transferrin receptor impairs T cell metabolism and function in systemic lupus erythematosus. *Sci Immunol*. 2023;8:eabq0178. doi:10.1126/sciimmunol.abq0178
30. Chen Q, Wang J, Xiang M, et al. The potential role of ferroptosis in systemic lupus erythematosus. *Front Immunol*. 2022;13:855622. doi:10.3389/fimmu.2022.855622